UNIVERSITY OF CALIFORNIA, SAN DIEGO

Characterization of Caspase-8 and p85alpha in Ovarian Cancer

A Thesis submitted in partial satisfaction of the requirements
for the degree Master of Science

in

Biology

by

Lauren Elizabeth Chen

Committee in charge:

Professor Dwayne G. Stupack, Chair
Professor Stephen M. Hedrick, Co-Chair
Professor Katherine A. Jones

2014

The Thesis of Lauren Elizabeth Chen is approved, and it is acceptable in quality and form for publication on microfilm and electronically:

Co-Chair

Chair

University of California, San Diego

2014

DEDICATION

I dedicate this thesis to my family and friends. Especially my parents, D.K. Chen and C.H. Chen, MD, for their love and support throughout my studies in science. My brothers Ryan and Nolan, who have encouraged me every step of the way. Also I give special thanks to my friends who have provided joy and memories throughout the many stressful times of my studies.

Additionally, in recognition of the members of the Stupack lab for their guidance and help in this project – Dr. Dwayne G. Stupack for his mentorship and giving me the opportunity to conduct meaningful research; Dr. Nadine Keller, for her supervising me with unwavering patience, motivating me to always do better, and answering all of my many questions; and to the rest of the Stupack lab whose support, wisdom, and camaraderie I will always remember.

In recognition of Dr. Stephen Hedrick and Dr. Katherine Jones for serving on my thesis committee, I sincerely appreciate your time and support of my master's thesis.

TABLE OF CONTENTS

LIST OF ABBREVIATIONS

Apaf-1	Apoptotic protease activating factor 1
BAK	Bcl-2 homologus antagonist killer
BAX	Bcl-2 associated X protein
Bid	BH3 interacting-domain death agonist
C8	Caspase-8
C8i	Inactive caspase-8 (C360A)
CA-125	Cancer antigen 125
CT	Computerized tomography
DED	Death effector domain
DISC	Death inducing complex
DNA	Deoxyribonucleic acid
EGF	Epidermal growth factor
ELISA	Enzymed linked immunosorbent assay
FADD	Fas-associated protein with death domain
GAP	GTPase activating protein
GEF	Guanine nucleotide exchange factor
HSQC	Heteronuclear single quantum coherence spectroscopy
IRS-1/2	Insulin receptor substrate 1 or 2
MEFs	Mouse embryonic fibroblasts
MRI	Magnetic resonance imagine
PDGFR	platelet derived growth factor receptor
PI(3,4,5)P3	Phosphatidylinositol 3,4,5-triphosphate
PI(4,5)P2	Phosphatidylinositol 4,5-bisphosphate
PI3K	Phosphoinositide-3-kinase
SH2 domain	Src homology 2 domain
t-Bid	Truncated BH3 interacting-domain death agonist
TNFα	Tumor necrosis factor
TRADD	Tumor necrosis factor receptor-associated death domain protein
TVUS	Transvaginal ultrasound

LIST OF FIGURES

ACKNOWLEDGMENTS

This work in part includes material currently being prepared for publication: Keller, Nadine; Chen, Lauren E.; Opella, Stan; Stupack, Dwayne G., “Caspase-8 interactions with the nSH2 domain of p85alpha to regulate cell adhesion in ovarian cancer”. In addition data from ELISA described in this work have been published: Graf, R., Barbero, S., Keller, N., Chen, L., Uryu, S., Schlaepfer, D., Stupack, D., *Src-inducible association of CrkL with procaspase-8 promotes cell migration.* Cell Adh Migr. **7**(4): p. 362-9.

ABSTRACT OF THE THESIS

Characterization of Caspase-8 and p85alpha in Ovarian Cancer

by

Lauren Elizabeth Chen

Master of Science in Biology

University of California, San Diego, 2014

Professor Dwayne G. Stupack, Chair
Professor Stephen M. Hedrick, Co-Chair

Caspase-8 is a cytosolic cysteine protease that induces programmed cell death by processing a variety of apoptotic substrates [1]. Conversely, it has been shown to have non-apoptotic functions and is upregulated in many cancers, including ovarian cancer [2, 3]. In neuroblastoma cells, post-translational modification of caspase-8 by tyrosine phosphorylation has been shown to promote cell adhesion and migration, which are hallmarks of cancer cells [2, 4, 5]. Phosphorylated tyrosine residues may bind to SH2 (src homology 2) domains, which are present in 121 human proteins, and may be involved in

caspase-8 dependent migration. The regulatory subunit of PI3K (phosphoinositide-3 kinase) p85α contains two SH2 domains, and has been previously suggested to be involved in migration [2]. Here, I characterize a direct and typical SH2-phosphotyrosine interaction between the Y380 of caspase-8 and the nSH2 domain of p85α in ovarian cancer cells. In addition, caspase-8 appears to promote adhesion in ovarian cancer cells, but potentially in a manner that is independent of the Y380 site. Protein modeling of caspase-8/p85α/p110α reveals potential mechanisms in which such an interaction could affect PI3K signaling. Understanding the implications of a caspase-8 and p85α interaction may further clarify the mechanisms by which caspase-8's dual roles are regulated, providing insight into the paradoxical retention of the caspase during tumor progression, as well as for therapies directed at optimizing tumor cell death.

INTRODUCTION

Cancer: a brief history

As of 2013, average estimates indicate that one in two men and one in three women have a lifetime risk of developing cancer [6]. However, cancer is not a recent disease. Evidence of cancerous growths has been found on fossilized mummies and bones from ancient Egypt. In 460-370 BC, Hippocrates termed the disease *karkinos* which later was translated into *cancer*. In 130-200 AD, Galen, a Greek physician, termed the study of cancer *oncology* based on the Greek word for swelling *oncos* [7, 8].

Throughout the sixteenth and eighteenth centuries, the performance of autopsies led to the development of cancer surgery, similar to how tumor resections are done today [7]. The development of the microscope in the nineteenth century brought clinicians and scientists together to study the pathology of cancer. Continuing to the twenty-first century, technological advances have furthered our knowledge of basic biology and in turn, how cancer develops. For example, the discovery of DNA's chemical structure by Watson and Crick led to today's understanding of DNA as the basis of the genetic code [9]. Scientists quickly concluded that external factors (radiation, chemicals, and viruses) that damage genes and some internal factors (inheritable mutations, hormones, and immune conditions) can cause cancer.

Throughout the world, 14.1 million adults were diagnosed and 8.2 million died from cancer in 2012 [7]. If incident and mortality trends continue, those affected by cancer will increase to 23.6 million each year by 2030 [6]. In the United States, cancer is the second leading cause of death, where it accounts for almost one in four deaths [10] (Figure 1).

1. Lung & Bronchus	72,330	26%
2. Breast	40,000	15%
3. Colorectum	24,040	9%
4. Pancreas	19,420	7%
5. Ovary	14,270	5%
6. Leukemia	10,050	4%
7. Uterine corpus	8,590	3%
8. Non-Hodgkin Lymphoma	8,520	3%
9. Liver & intrahepatic bile duct	7,130	3%
10. Brain & other nervous system	6,230	2%
All Sites (2014)	275,710	100%

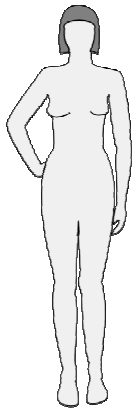

Figure 1: Cancer statistics

Listed are the ten leading cancer types by death. [10]

While there are many types of cancer, all are characterized by an uncontrollable growth of abnormal cells with the malignant ability to invade and spread into normal tissues. Abnormal cells arise from normal cells that have DNA damage, whether from external carcinogens or inheritable mutations affecting tumor suppressor genes and oncogenes. While normal cells with DNA damage undergo repair or eventually die, abnormal cells continue to proliferate, accumulate more mutations, and eventually become malignant (reviewed in [7]).

A key difference between normal cells and cancerous cells is their ability to metastasize to other tissues (Figure 2). Tumor metastasis is initiated when cancer cells from the primary tumor invade into surrounding tissues and intravasate (move into vessels) through the walls of lymph or blood vessels [11]. Circulating in lymph or blood vessels, tumor cells may stop moving in distant capillaries and extravasate (move out of the vessels) into nearby tissues [11]. Once arrested in a distant tissue, tumor cells may proliferate and form small tumors called micrometastases (micromets) [11]. Micromets

promote self-growth via angiogenesis, the formation of blood vessels, to gain access to nutrients and oxygen from the blood [11].

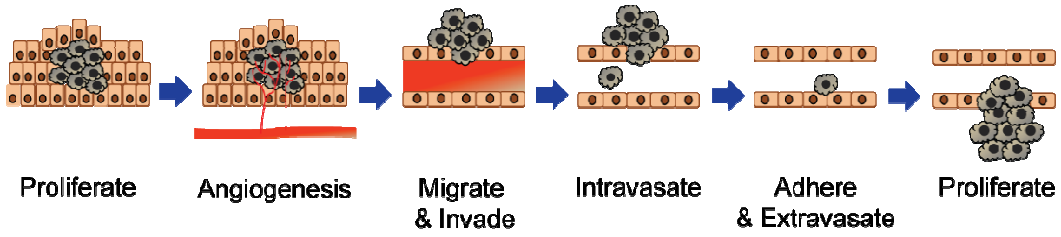

Figure 2: Key cell functions in metastasis

Adapted from [12]

Ovarian Cancer

Ovarian cancer is the fifth leading cause of cancer related deaths in women in the United States, accounting for the most deaths of any other female reproductive cancer [6] (Figure 1). In 2011, 188,867 women in the United States were living with ovarian cancer [13]. In 2014 alone, there will be an estimated 21,980 new cases of ovarian cancer and 14,270 deaths [14]. Of all ovarian tumors, 85-90% generally originate from epithelial cells that line the ovary, while fewer tumors originate from germ cells that produce the ova and eggs and stromal cells that hold the ovary together [13]. While patients with germ cell and stromal cell tumors have a 90% survival rate over five years and more than 75% of patients surviving long term, most ovarian cancers are epithelial and highly malignant [13].

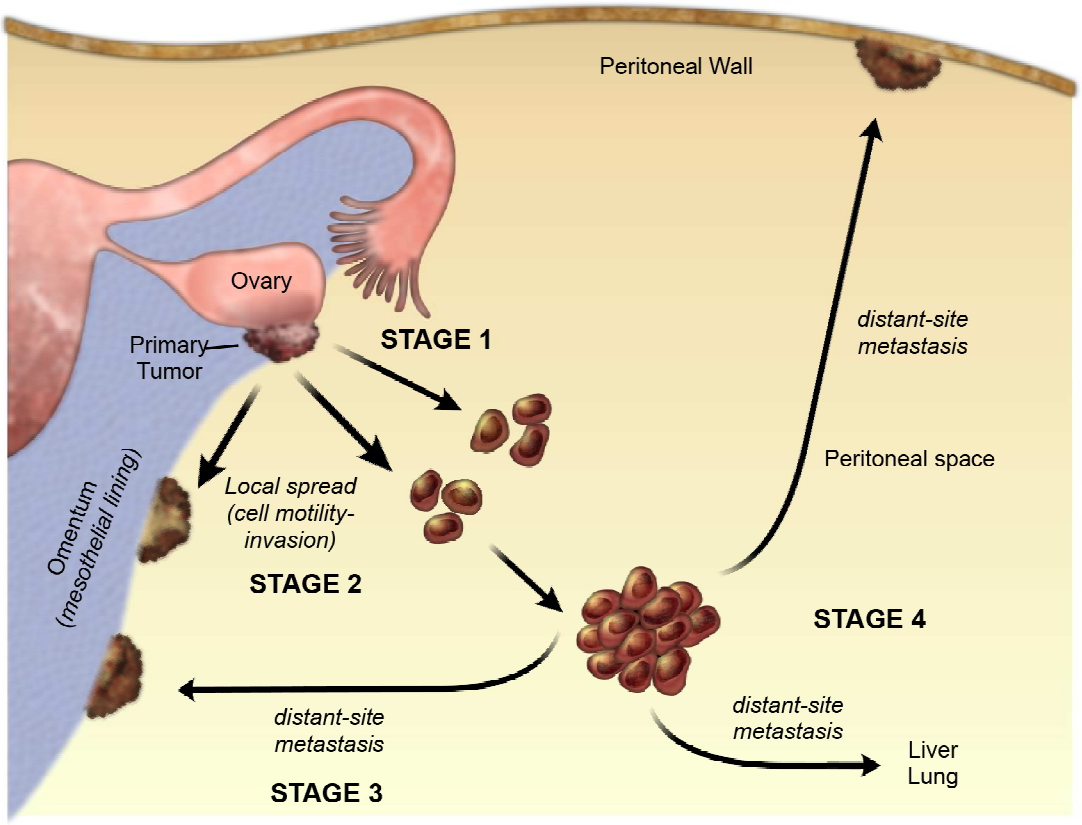

Figure 3: Ovarian cancer staging

Adapted from [15]

Ovarian cancer progresses in several stages, which are defined as follows: (Figure 3) local tumorigenesis limited to the ovaries (stage I), tumorigenesis extended to the pelvic region (stage II), to outside of pelvis (stage III), and to distant tissues (stage IV), most commonly the liver, lung, and peritoneum [11, 16]. Whereas only 15% of ovarian cancers are found at stage I, of which 92% have a five year survival rate, 61% of women with ovarian cancer are diagnosed with late staged cancer that has progressed to distant tissues, which has a significantly diminished five year survival rate of 27% [14]. Detecting early ovarian cancer is challenging because initial symptoms are vague and

similar to that of other gastrointestinal conditions [17]. Common signs such as bloating, pelvic and abdominal pain, difficulty eating, urinary urgency, fatigue, and swelling can be symptoms of benign illnesses, but when due to ovarian cancer may persist for a few weeks. Moreover, unlike breast cancer where mammograms can detect cancers early on in people without symptoms, similar tests such as the transvaginal ultrasound (TVUS) or the CA-125 blood test for ovarian cancer have not been as successful as these screens have not proved to lower the number of ovarian cancer deaths [13]. To detect cancerous masses, noninvasive imaging procedures (ultrasound, CT, and MRI) or pelvic exams are used [13]. Typically, a sample of the tumor or built up fluid from the tumor (ascites) will be taken for a pathologist to classify and help to diagnose.

Treatment strategies for ovarian cancers generally include a combination of cytoreductive surgery to remove as much tumor as possible or complete removal of the ovaries and fallopian tubes, followed by radiation or chemotherapy to kill remaining cancer cells. Usually chemotherapy treatments for ovarian cancer combine a platinum based (i.e. cisplatin or carboplatin) and a taxane based (i.e. paclitaxel) therapy [18, 19]. However, due to the heterogeneity of mutations in ovarian cancer, there are often small populations of cells resistant to chemotherapy drugs. While resistant cells are sometimes dormant, they more often develop into malignant cancers due to the inability to treat the cells with chemotherapy [19]. Evidence of this recurrence phenomenon due to drug resistance occurs in up to 75% of patients who are treated with cisplatin, many of whom eventually succumb to the disease [20].

Because ovarian cancer is usually diagnosed at later stages, understanding what contributes to tumor development and metastasis is important for ovarian cancer research.

Frequently, pathways that affect cellular functions such as migration, invasion, adhesion, proliferation, apoptosis, and angiogenesis, are altered in tumor biology and are important for cancer research [21] (Figure 2). For instance, specific genomic and proteomic aberrations in the regulation of apoptosis (programmed cell death) have been associated with the development of invasive epithelial ovarian cancers [22].

Caspase-8 as a key player in apoptosis

Whereas apoptosis is downregulated in cancer, it is critical for maintaining and developing healthy tissues. By balancing cell division and apoptosis, multicellular organisms can reduce, increase, or stabilize the number of cells in tissues. Compared to necrotic cell death where cells swell and release their intracellular components into the extracellular space, apoptosis is a highly regulated process where cells shrink, collapse, and bleb into easily phagocytosed fragments. Thus apoptosis is not as damaging as necrosis, and allows for dead cellular material to be recycled by other cells. However, disruptions in the apoptotic machinery can be the basis for many diseases. Gain of function mutations that cause overactive apoptosis may result in degenerative disease [23]. In contrast, loss of function, evasion, or resistance to apoptosis can be the pathological basis for the development of cancer.

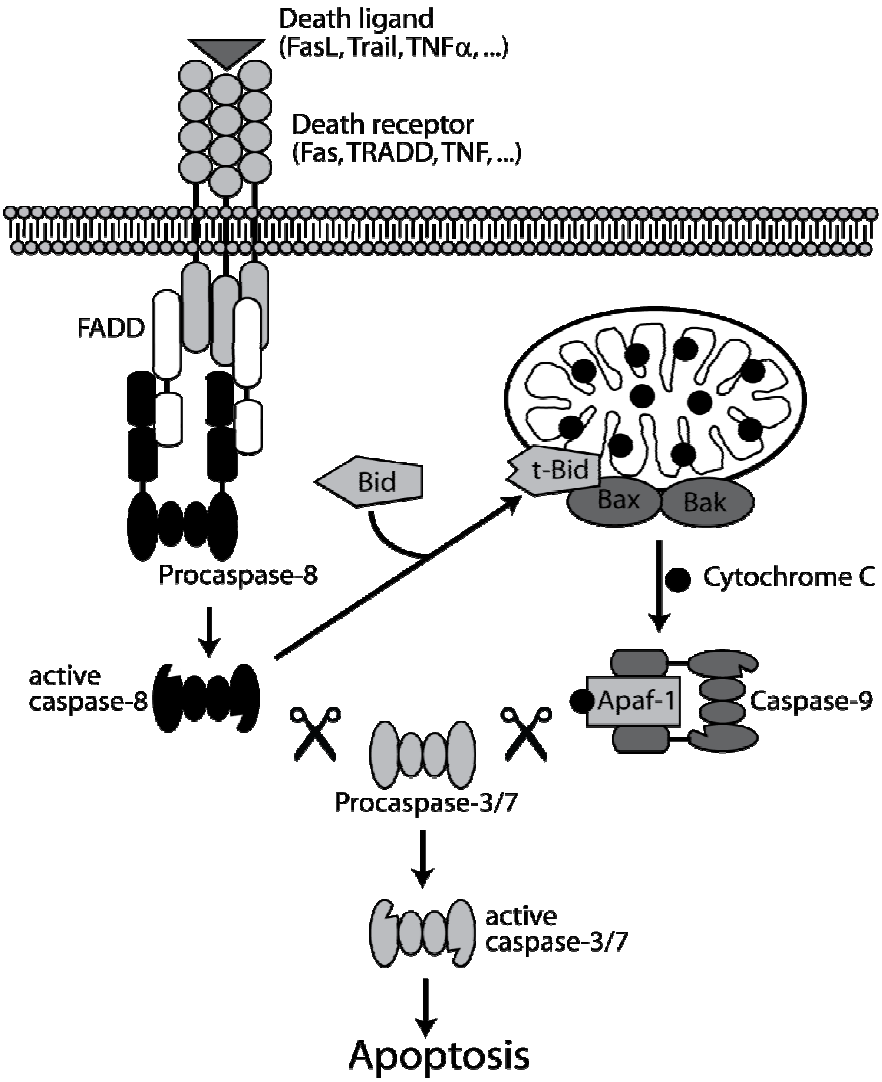

Figure 4: Intrinsic and extrinsic apoptosis pathway

Reproduced with permission from N. Keller

Central to the apoptotic pathway is the protein caspase-8, which belongs to a family of proteins called caspases, aptly named for their cysteine dependent aspartate cleaving protease abilities. Its main role is as initiator caspase in the extrinsic apoptotic pathway (Figure 4). When a death ligand binds to a death receptor, it triggers the formation of a death inducing complex (DISC) including adaptor proteins (i.e. FADD),

which recruits inactive monomeric pro-caspase-8 to the membrane via its two death effector domains (DEDs) [24]. Upon dimerization through induced proximity, procaspase-8 undergoes conformational changes and autoprocesses, thereby severing the DEDs from the catalytic domain as well as removing the intersubunit linker between the catalytic p18 and p11 subunits [25-27] (Figure 5). The resulting active caspase-8 processed dimer is freed from the membrane and able to cleave and activate downstream inactive dimeric executioner caspases, such as caspase-3. Once activated, caspase-3 cleaves a big variety of substrates, which ultimately results in apoptotic cell death.

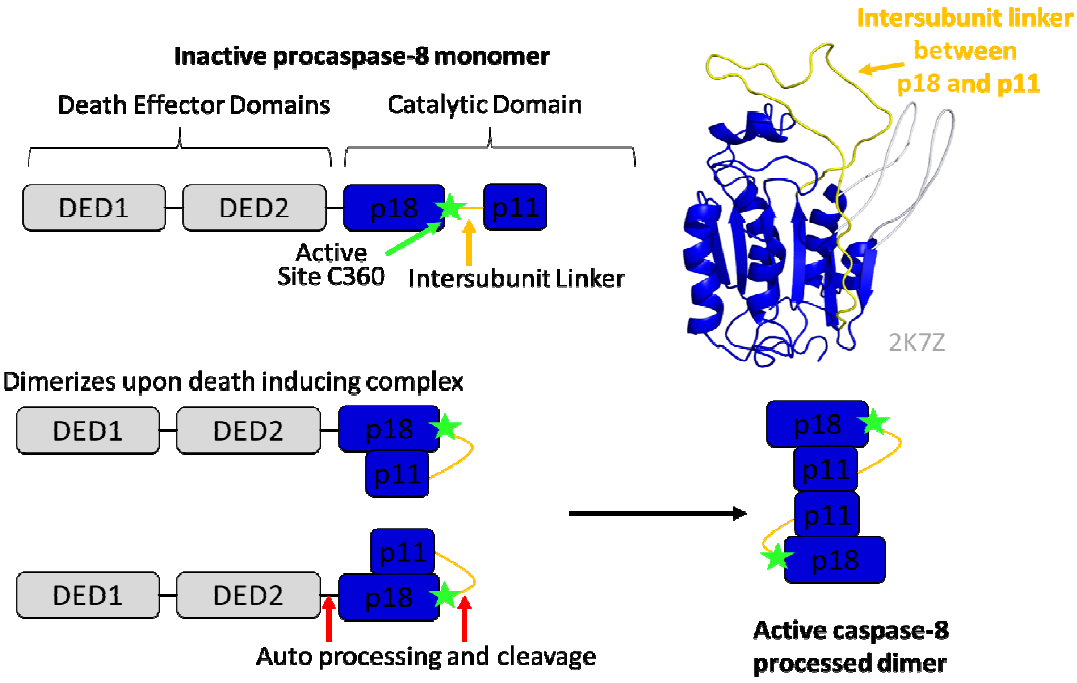

Figure 5: Dimerization and activation of caspase-8

Besides the extrinsic apoptotic pathway, caspase-8 can also induce the intrinsic mitochondrial pathway (Figure 4). Active dimeric caspase-8 can cleave the Bcl-2 family protein Bid, to form truncated Bid (tBid), which results in conformational changes in Bax/Bak and subsequent release of cytochrome C and other pro-apoptotic factors from the mitochondria [28]. Together with Apaf-1 and initiator caspase-9, cytochrome C forms a macromolecular complex called the apoptosome, which serves as an activation platform for caspase-9. Activated caspase-9 cleaves and activates capase-3, which then induces downstream apoptotic signaling.

Caspase-8 as a regulator of cell survival

Even though caspase-8 is an initiator of apoptosis, it has been seen upregulated in multiple cancers, including ovarian cancer, indicating that it may have non-apoptotic functions [2, 3] (Figure 6). In fact, homozygous caspase-8 knockout mice are embryonically lethal, with impaired cardiac development and diminished hematopoietic recovery, suggesting that caspase-8 is vital for embryonic development [29]. Caspase-8 has also been found to have non-apoptotic functions such as promoting cell migration and survival, traits associated with cancer metastasis. For instance, caspase-8 induced migration and caspase-8 involvement in calpain activation was seen in mouse embryonic fibroblasts (MEFs) [30]. Moreover, caspase-8 was able to promote migration by interacting with calpain 2 and focal adhesion kinase to encourage cleavage of focal adhesion substrates in neuroblastoma NB7 cells [31]. Whereas catalytic activity is required for an apoptotic role of caspase-8, it seems to be dispensable for its non-apoptotic functions. How caspase-8 is able switch between these two seemingly opposing

roles, is of interest to cancer research. Clarification of the mechanisms underlying this switch would assist in developing cancer therapies targeted at only one of the pathways caspase-8 is involved in without affecting its other functions.

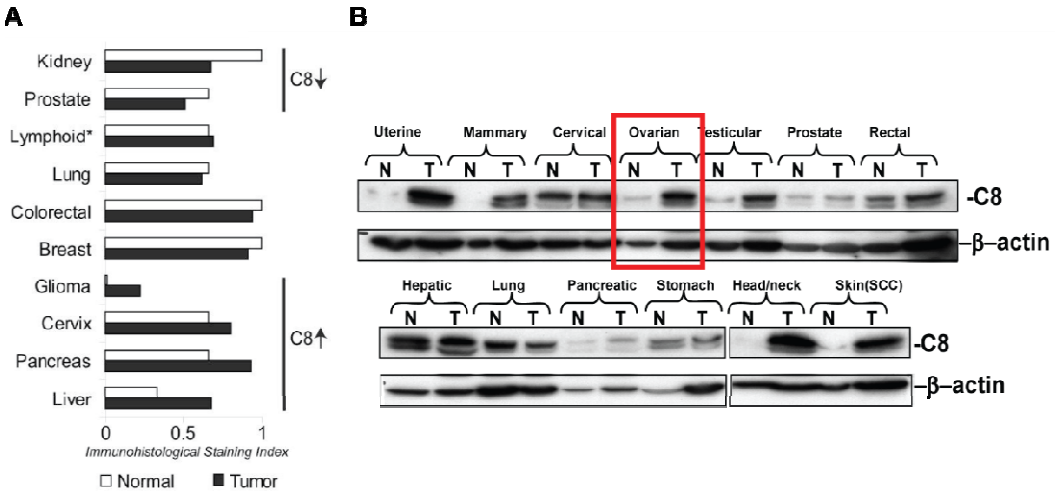

Figure 6: Caspase-8 is upregulated in cancer

Reproduced with permission from D. Stupack, UCSD S. Frisch WVU [2, 3]

Tyrosine phosphorylation as a regulator for caspase-8 function

There is accumulating evidence that posttranslational modifications, such as phosphorylation of tyrosine (Y) residues, affect the role caspase-8. For instance, Y380 phosphorylation of caspase-8 by Src kinase was shown to inhibit Fas-induced apoptosis [32]. Additionally, caspase-8 was found to promote cell migration dependent on the phosphorylation of Y380 and independently of catalytic activity [4]. Mechanistically, molecular studies of caspase-8 activation showed that the cleavage rate of phosphorylated caspase-8 was reduced compared to unphosphorylated caspase-8 [25, 32]. Y380 is located within the intersubunit linker of caspase-8 and is removed during enzymatic

maturation. Phosphorylation at this residue may alter the intersubunit linker conformation or sterically hinder cleavage [25].

Furthermore, it has been shown that phosphorylation of tyrosine residues on caspase-8 promotes protein-protein interactions, in particular with protein domains belonging to the class of src homology 2 (SH2) domains.

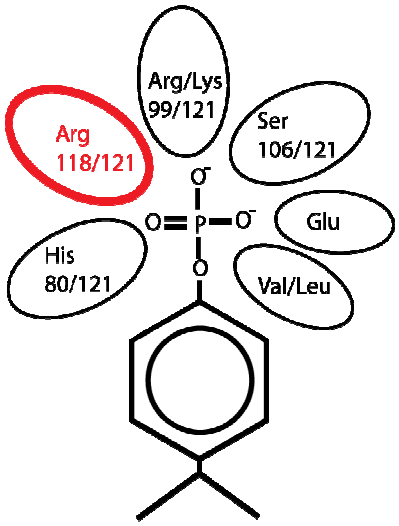

Figure 7: SH2 domain conserved residues in the phosphotyrosine binding pocket

Key conserved residues of the phosphotyrosine binding pocket, within each circle denoted in how many SH2 domains said residue is conserved out of 121 total human SH2 domains. Red circle indicates most conserved residue Arg [33].

Tyrosine phosphorylation and its interaction with SH2 domains

In the human genome, 111 genes have at least one src homology 2 (SH2) domains, with a total of 121 individual SH2 domains expressed (reviewed in [33]). These domains are highly conserved in structure, all having two α-helices sandwiching an anti-parallel tripled stranded β-sheet [34]. SH2 domains contain a binding pocket that can accommodate a phosphorylated tyrosine and three to five amino acids c-terminal to the

tyrosine [33]. The residues that make up the phosphotyrosine binding pocket are highly conserved among all 121 SH2 domains: Arg (118/121), Ser (106/121), Arg/Lys (99/121), and His (80/121) [33].The most conserved residue, Arg (118/121), lies in the βB structure, and provides a positive charge that stabilizes binding with the negative phosphotyrosine [33] (Figure 7).

Tyrosine phosphorylated caspase-8 has previously been shown to bind to proteins with SH2 domains. For example, Tyrosine phosphorylation by Lyn (Y380 and Y448) of caspase-8 was shown to inhibit neutrophil apoptosis [35]. Interestingly, SHP-1, which binds to phosphorylated Tyr293 via its SH2 domain, was shown to dephosphorylate caspase-8 at Y380, allowing neutrophil apoptosis to continue. Additional evidence was found using a neuroblastoma cell model, where the interaction of Src phosphorylated caspase-8 and the SH2 domain of CrkL, an adaptor protein associated with the regulation of cell survival and migration, promoted cell migration [35].

Caspase-8 and p85α

In line with accumulating support for non-apoptotic roles of caspase-8, is the finding that caspase-8 interacts with p85α to regulate cell adhesion and migration. Universally expressed in cells, p85α contains a src homology 3 (SH3) domain, a GTPase activating protein (Rho-GAP) domain, an inter SH2 (iSH2) domain, and notably two SH2 domains: an n-terminal SH2 (nSH2) and a c-terminal SH2 (cSH2) domain [36]. Specifically, Senft and colleagues used a caspase-8 peptide with a phosphorylated Y380 site to screen for binding in a protein chip array, containing 38 SH2 domains from various proteins, amongst them the N-terminal (nSH2) and C-terminal (cSH2) SH2

domains of p85α [2]. Together with domain deletion mutants of p85α used in pull down experiments, their data suggests that the cSH2 domain of p85α may be important for caspase-8 and p85α binding. Moreover, they characterized the interaction of caspase-8 Y380 as a regulator of cell adhesion and migration via functional assays using caspase-8-null neuroblastoma cells. This may indicate that the binding of p85α to caspase-8 is a mechanism by which caspase-8 toggles from apoptotic to cell survival functions

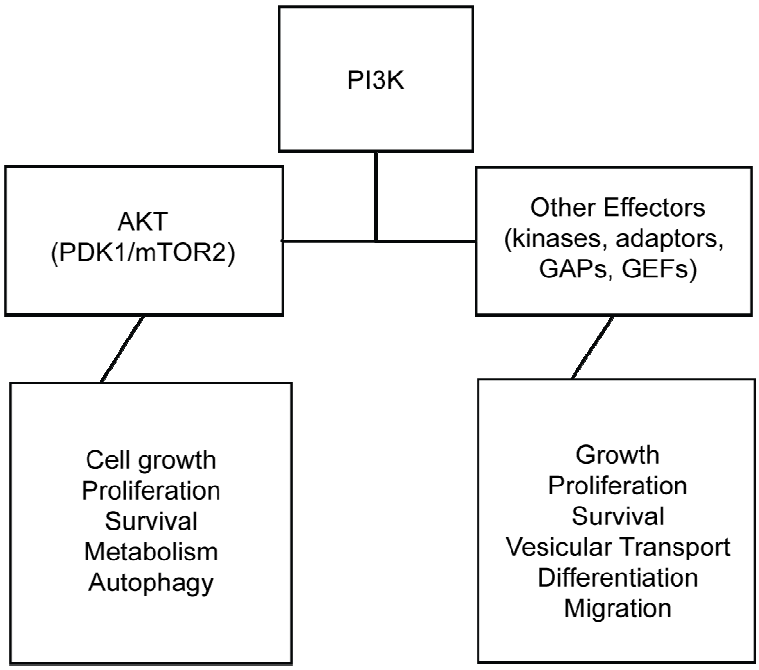

Figure 8: Cellular functions affected by PI3K signaling

Reviewed in [37]

The protein p85α is known as the regulatory subunit in phosphoinositide-3-kinase (PIP3), which binds to the catalytic subunit p110α. Several isoforms and splice variants of the regulatory and catalytic subunits exist, however the class I heterodimer p85α/p110α is the most studied to date. Overall, PI3K has been shown to regulate cell growth, survival, cell vesicle trafficking, migration, and proliferation (reviewed in [37])

(Figure 8). Taken together with the fact that PI3K signaling is upregulated in ~70% of ovarian cancers, p85α and its interaction with other proteins such as caspase-8 may play a crucial role in regulating the activation of downstream signal cascades carried about by PI3K in cancer [21].

Thesis aims

Senft and colleagues have detected an interaction between capase-8 and p85α that affects cell migration in neuroblastoma cells, potentially via up or down regulation of one of the many PI3K pathways. Perhaps this mechanism and complex will also be reflected in ovarian cancer models. This thesis aims to confirm the interaction by determining which domains and residues on caspase-8 and p85α are important for binding by mutating critical residues in both proteins. In addition to biochemical studies, the biological relevance of the capsase-8 and p85α interaction in ovarian cancer will be explored. We will propose a model of the caspase-8 and p85α interaction, which may clarify a non-apoptotic mechanism for caspase-8 in cancer. Deeper understanding of exactly how caspase-8 toggles between cell killing versus cell survival roles is critical in establishing caspase-8 as a target for developing cancer therapies.

METHODS

Materials

The following antibodies were used: anti-caspase-8 (BD BioSciences 551242, GeneTex GTX100905, serum raised in rabbits), anti-p85a cSH2 domain (BD BioSciences 610045), BD anti-p85α (Santa Cruz sc1637), anti-phosphotyrosine (Millipore 05-321), anti-GST (raised in rabbits), anti-p110a (cell signaling, 4255S), anti-pAKT Ser473 (cell signaling 4060), anti-t-AKT (cell signaling 9272), anti-actin (Sigma A5441), anti-tubulin (Calbiochem CP06), anti-mCherry (raised in rabbits and purified). Secondary antibodies were obtained from Fischer Scientific (DyLight goat anti-mouse 680nm (PI35518) and goat anti-rabbit 800nm (PI35571)) and Jackson ImmunoResearch (goat-anti-rabbit HRP (111-035-003) and goat-anti-mouse HRP (115-035-003)), Invitrogen (Alexa Fluor 488 goat anti-mouse (A11001), Alexa Fluor 647 goat anti-rabbit (A-21245)). Alexa Fluor 633 phalloidin (A22284) and DAPI (D-1306) were obtained from Life Technologies and Molecular Probes, respectively.

Generation of DNA constructs

Full length bovine p85α and caspase-8 were cloned between the NheI and EcoRI restrictions sites of the mammalian PCDH expression vector containing an n-terminal mCherry tag or GFP tag, respectively. Single domain SH2 constructs (M322-Y431 for nSH2 and M614-R734 for cSH2) were cloned between BamHI and EcoRI into the bacterial expression vector pGEX 4T2 vector (GE Healthcare). Constructs for the catalytic domain of caspase-8 were established previously [26]. Site directed mutagenesis was used to generate the R358A mutant of p85α and C360A (C8i) and tyrosine mutants.

Protein purification

Inactive caspase-8 (C8i) tyrosine mutants were purified as described previously [26]. GST pGEX 4T2 nSH2, nSH2 R358A, and cSH2 constructs were expressed in BL21(DE3) pLysS cells in LB. Cells were grown overnight, harvested, resuspended in fresh LB with ampicillin, induced to express protein with IPTG with a final concentration of 0.8mM for 3hrs. Bacteria was pelleted, resuspended in cold PBS with DNAse (Sigma DN25-100), and lysed by sonication (3 times 30 cycles, duty cycle 50%). Lysate was centrifuged, and the supernatant was filtered, then allowed to batch incubate with glutathione-sepharose slurry (Fischer, 45000139) for 2hrs at 4°C. Sepharose beads were loaded into a column, washed with 10 CV PBS, 5 CV of a high salt buffer, PBS, and eluted into 1 ml fractions with buffer. Fractions were pooled based on Commassie stained SDS-PAGE and dialyzed against PBS. 10% glycerol was added and the protein stored at -80°C .Protein concentration was determined via Micro BCA protein assay kit (Pierce, 23228).

***In vitro* caspase-8 phosphorylation and ELISAs**

Purified caspase-8 protein was incubated in Src reaction buffer (see appendix) and incubated at 32°C for 1h. A96-well plate was coated with bait protein (1uM) for 2hrs at 37^{o}C. Unbound protein was removed and the plate was blocked with 5% milk in TBST for 2hrs 37^{o}C. Wells were washed with TBST, and the second protein was added (0.1uM) for 2hrs at 37^{o}C. Unbound proteins were removed by washing 3 times with TBST. The plate was incubated with the appropriate primary antibody diluted in TBST for 1hr at

37^{o}C. Wells were washed 3 times and incubated with goat anti rabbit HRP-conjugated secondary antibody for 1hr at 37^{o}C. Wells were washed with TBST, presence of the second protein was detected by addition of TMB substrate(Millipore) and subsequent calorimetric analysis at 600nm using a Bio Tek plate reader. A second wavelength of 450nm was used as a reverence wavelength.

Cell culture

HEK 293T cells were cultured in high glucose (4.5 g/L) Dulbecco's modified Eagle's medium (DMEM) supplemented with 10% fetal bovine serum (Gibco), 1% non-essential amino acids, antibiotic antimyotic (Mediatech) at 37°C, 5% CO_2. OVCAR5 and SKOV3 cells were cultured in RPMI 1640 L-glutamine (Life Technologies) supplemented with 10% FBS (Omega), 1% non-essential amino acids, 1% sodium pyruvate, and antibiotic antimyotic (Mediatech) at 37°C, 5% CO_2.

Caspase-8 knockdowns and reconstitutions

Knockdown virus was made by transfecting HEK 293T cells. Briefly, cells were seeded at 1.6 million/6-well for 24 hrs and transfected with 1.5 µg packaging vectors (pRSV-REV, pCMV-VSVG, pMDLg/pRRE; 0.5 µg/µl each), desired DNA construct(1.5 µg), and Lipofectamine2000 (7.5 µl) (Invitrogen) diluted in 250 µl Opti-mem (Life Technologies). The transfection media was removed after 12-16hrs and replace with 3 ml DMEM complete. After 48hrs, virus containing supernatant was collected , floating cells removed and virus frozen at -80ºC. OVCAR5 or SKOV3 cells were infected with 1ml virus in complete media containing polybrene (8 µg/ml) and centrifuged at 1600 rpm for

1 hr at room temperature. After 48 hours, selection drugs puromycin (VWR) or blasticidin (Invitrogen) was added 1:1000 to select stable cell lines.

Western blotting

Samples were resolved on 10% or 15% SDS-PAGE using running buffer, and wet transferred with transfer buffer onto PVDF immobilon-FL. Proteins were detected either by fluorescence using an Odyssey imager (LiCor) or by chemiluminescence (Thermo Scientific) and development using autoradiography film (Genesee Scientific). For development on film membranes were blocked with 5% milk in TBST. Primary and secondary HRP antibodies were diluted in blocking buffer. For development by fluorescence signal the membranes were blocked with 0.1% casein in PBS and the primary and secondary Dylight antibodies were diluted in PBST.

Immunofluorescence

HEK 293T cells were transiently transfected with FuGENE HD according to Promega protocol database. Briefly, cells were seeded $1x10^6$ in a 60mm dish in 6ml complete media. Fugene HD : DNA ratio used was 3:1 at 6.5ug DNA per dish, diluted in OptiMem, and incubated at room temperature for 10minutes. Complex was added dropwise to cells. After 48hrs, transfected cells were seeded onto coverslips precoated with 2ug/ml fibronectin, adhered for 2hrs, fixed with 4% paraformaldehyde in PBS for 10 minutes, permeabilized with 0.1% Triton X-100 in PBS for 2 minutes, and blocked in 5% BSA in PBS. Primary antibodies for p85α and caspase-8 were diluted in blocking buffer and added to coverslips for 2hrs. After washing with PBS secondary antibodies diluted in

blocking were added to coverslips for 2hrs. The secondary antibodies were removed and phalloidin and DAPI stains diluted in blocking buffer were added for 30min. Coverslips were mounted using Vectashield hardset mounting medium (Vector) onto coverslides. Images were taken with a Nikon Eclipse C1 confocal microscope with EZ-C1 3.50 imaging software at 100x oil immersion lens with a minimum pinhole (30um).

Immunoprecipitation and pull downs

Cells were seeded for 24 hrs, starved for 16 hrs, and treated for 1 hr with EGF stimulation media (see appendix). Attached cells were washed with PBS and lysed in RIPA buffer. Protein concentration determined by Micro BCA protein assay (Pierce). 1000 µg of protein was diluted in TBS 1% NP-40 and incubated with 2.5 µg anti-mCherry polyclonal antibody or GST fusion protein, rotating for 2hrs at 4°C. Complexes were precipitated with protein A or glutathione sepharose beads, respectively for 2 hrs at 4ºC. Beads were washed 5 times in TBS 0.1% NP-40, resuspended 10 µl in 6x Commassie reducing buffer.

Adhesion Assay

Non-TC treated 48-well plates were coated with fibronectin for 1 hr, then blocked with 3% BSA in PBS for 1 hr at 37°C. Cells were added in serum free DMEM, allowed to attach for 1hr. Non-attached cells were removed and attached cells were fixed and stained by addition of crystal violet staining solution for 30 min. Excess crystal violet was removed by washing with water and the plates were tried. For quantification of

crystal violet uptake the stain was extracted by addition of methanol calorimetric analysis at 600nm using a Bio Tek plate reader.

Modeling of p85α/p110/caspase-8 complex

Models of protein-protein interaction between caspase-8 and nSH2 as well as caspase-8 with PI3K were generated using PyMol. To model the caspase-8 nSH2 complex the intersubunit linker containing Y380 of caspase-8 (pdb: 2K7Z) was aligned with a phosphopeptide bound to the nSH2 domain of p85α (pdb: 2IUG). The structure of PI3K is a combination of the individual crystal structures of p110a with the nSH2-iSH2 fragment of p85α (pdb: 4L1B) and p110 with the iSH2-cSH2 fragment (pdb: 2Y3A). The approximate position of caspase-8 in respect to the PI3 kinase was predicted by alignment of the caspase-8 nSH2 model with the nSH2 of the PI3 kinase.

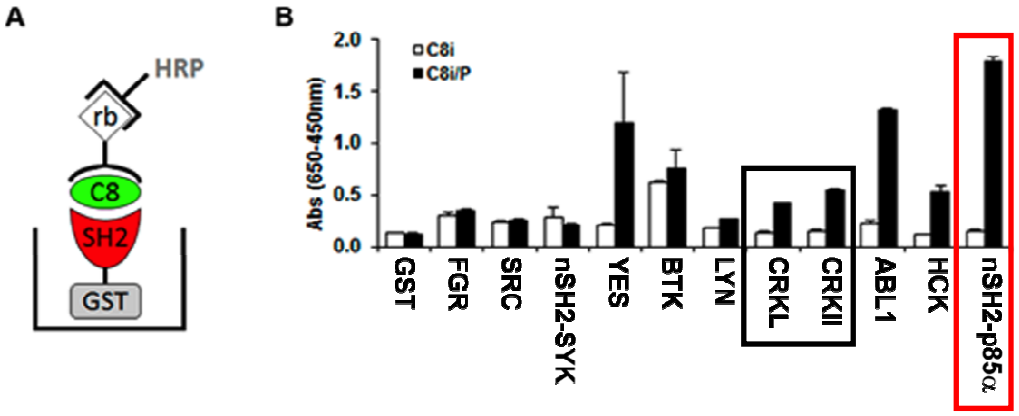

Figure 9: Phosphorylated caspase-8 binds to various SH2 domains

A) ELISA scheme indicating bait as GST-tagged SH2 protein for B. B) Purified catalytic domain of caspase-8 was phosphorylated by Src kinase *in vitro* and screened for binding to various GST-tagged SH2 domains via ELISA. Black boxed data was incorporated into Graf et al. 2013. Red boxed data indicates highest binding

Phosphorylated caspase-8 binds to SH2 domains

To identify novel interaction partners for phosphorylated caspase-8, a library of SH2 domains was screened with inactive caspase-8 catalytic domain in an ELISA (Figure 9 A, B). Since Src kinase was shown to phosphorylate caspase-8 tyrosine residues [32], purified catalytic domain of caspase-8 was phosphorylated *in vitro* with recombinant Src kinase. GST-tagged nSH2 and cSH2 domains were used as baits for inactive caspase-8. Caspase-8 interacted with several SH2 domains in a phosphorylation-dependent manner, as assessed by using a nonphosphorylated caspase-8 as control (Figure 9 B). Phosphorylation of caspase-8 did not induce binding to the SH2 domains of FGR, SRC, BTK, and the nSH2 domain of SYK. However, it showed increased binding affinity to LYN, CrkL, CrkII, Abl1, HCK, and p85D1 with the nSH2 of p85α displaying the

strongest signal. Data from this screen was incorporated into a figure supporting novel interactions between caspase-8 and CrkL and CrkII in Graf et al. (2013).

Caspase-8 is phosphorylated primarily on Y380

To investigate the effect of phosphorylation of tyrosines on caspase-8 further, our lab used prediction analysis programs, mass spectra analysis, and structural analysis of the catalytic domain to determine 5 tyrosine residues that are can be phosphorylated and are exposed to the surface or pockets: Y324, Y334, Y380, Y412, and Y448 (unpublished results, Figure 9 A). Selected tyrosines were individually mutated to phenylalanine to generate the inactive caspase-8 mutants: Y324F, Y334F, Y380F, Y412F, Y448F, and Y5F (in which all five Tyr are mutated to Phe). Mutants were expressed, purified, and phosphorylated *in vitro* by purified Src kinase. Levels of tyrosine phosphorylation were determined by western blot and quantified (Figure 9 B, C). Phosphorylation of caspase-8 drastically decreased for the Y380F mutant and slightly more for the Y5F caspase-8 mutant, indicating that Y380 is the major but not the only tyrosine phosphorylated by Src.

Y380 of caspase-8 binds to the nSH2 domain of p85α

Since the initial ELISA screen of SH2 domains only included the nSH2 but not the cSH2 domain of p85α, we performed ELISAs using both SH2 domains and the purified caspase-8 tyrosine mutants (Figure 9 D). An interaction between caspase-8 and the cSH2 domain has been previously described [2]. Surprisingly, the cSH2 domain of p85α did not bind to caspase-8 or any of the tyrosine mutants, regardless if phosphorylated or not. In contrast, significant binding of phosphorylated inactive

caspase-8 to the nSH2 domain was detected in wild-type and all but the Y380F and Y5F mutants, indicating that phosphorylation of Y380 is critical for the binding to the nSH2 domain of p85α. To confirm that the lack of binding of the cSH2 domain is not due to improper protein folding, the proteins were isotope labeled and analyzed in a ^{15}N-HSQC NMR experiment (Figure 11). Broad peak dispersion in both protein spectra indicates that the nSH2 and cSH2 constructs used in the ELISA are properly folded.

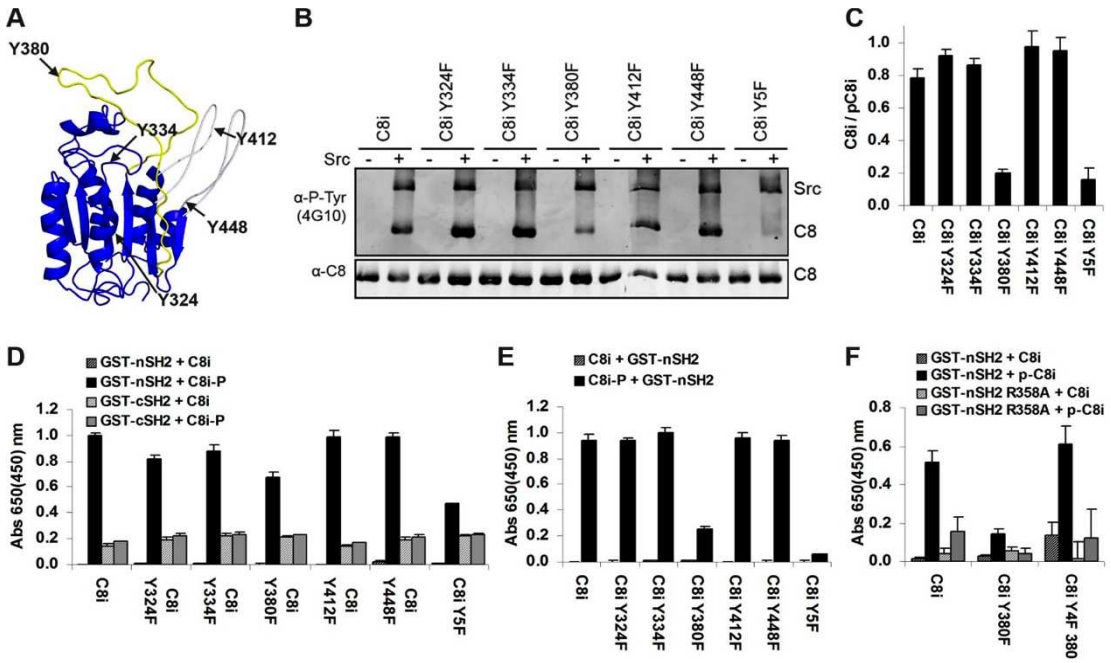

Figure 10: Caspase-8 tyrosine phosphorylation is mostly attributed to Y380

A) Solution structure of caspase-8 (pdb code: 2K7Z). Intersubunit linker is depicted in yellow, with arrows indicating surface tyrosines of B) Immunoblot of *in vitro* phosphorylation of capsase-8 with purified Src kinase. Total tyrosine phosphorylation of caspase-8 and Src is detected by αp-Tyr 4G10 antibody. C) Quantified ratio of phosphorylated caspase-8 over total caspase-8 from B. D,E) ELISA using phosphorylated caspase-8 mutants shown in C with either using GST bound SH2 domains or caspase-8 as bait. F) The nSH2 domain of p85α is sufficient and Arg358A is necessary for the interaction of nSH2 with phosphorylated caspase-8.

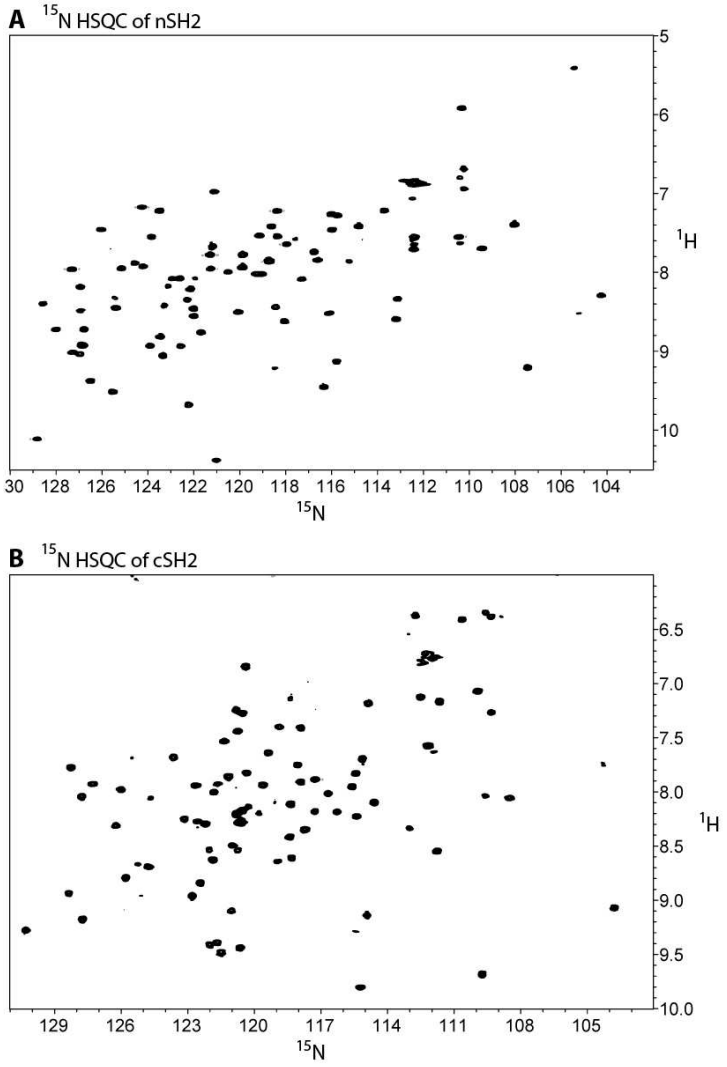

Figure 11: 15N-HSQC of nSH2 and cSH2

The DNA sequence coding for human p85α amino acids of nSH2 (A) and cSH2 (B) were cloned into PGEX 4T2 (GE Healthcare) with an N-terminal GST tag. For NMR analysis the GST-SH2 domains were expressed in M9 minimal media with 15N labeled ammonium sulfate and purified. The GST tag was removed by Thrombin cleavage and the SH2 domains dialyzed against 20 mM Tris, 100 mM NaCl and 1 mM TCEP. Spectra were recorded on a Varian500 at 305K.

To verify that the nSH2 domain of p85α binds to caspase-8 in an SH2-phosphotyrosine manner, an nSH2 R358A mutant was generated, in which the highly conserved arginine that stabilizes phosphotyrosine interaction in the binding pocket was

changed to an alanine. An ELISA screen comparing the binding ability of GST-tagged nSH2 to nSH2 R358A against inactive caspase-8 and inactive caspase-8 Y380F, demonstrates that caspase-8 indeed interacts with the nSH2 domain of p85α in a typical SH2-phosphotyrosine manner.

Caspase-8 and p85α interact in cells

Whereas ELISAs provide a defined system for determination of a direct protein-protein interaction, next whether such a complex is also formed intracellularly was investigated. HEK293T cells were transiently transfected with eGFP-tagged caspase-8 and mCherry-tagged p85α and analyzed via confocal microscopy (Figure 12). An enrichment of eGFP-tagged caspase-8 and mCherry-tagged p85α was seen along the cell periphery, of the spreading cells. This colocalization is distinct compared to the control transfection of either eGFP or mCherry alone, which produced an even distribution of fluorescence throughout the cell. Mutation of either Y380 or R358 still induced recruitment of the fluorescent-tagged proteins to the cell periphery. However, colocalization was not as apparent, as evident by more non-overlapping clusters and regions.

To further characterize the importance of R358 for the intracellular interaction of p85α with caspase-8 in an ovarian cancer model, endogenous caspase-8 was pulled down from OVCAR5 cells using purified GST-tagged SH2 domains and R358A mutant, respectively (Figure 13 A). To induce caspase-8 phosphorylation, OVCAR5 cells were stimulated with epidermal growth factor (EGF) and simultaneous Na_3VO_4 treatment, which was previously shown to stimulate endogenous caspase-8 phosphorylation [32].

The presence of either GST alone (control) or GST-tagged nSH2, nSH2 R358A and cSH2 was confirmed by Western blotting. Since the p85α antibody used only recognizes the nSH2 domain, the cSH2 domain was only detected by GST antibody. As expected, caspase-8 was not pulled down from the non-stimulated lysates. However, in EGF stimulated lysates, the nSH2 domain of p85α sufficiently pulled down caspase-8, while the cSH2 domain did not. In agreement with our previous ELISA results, the nSH2 R358A was unable to pull down caspase-8, indicating that complex formation was specific to an SH2-phosphotyrosine interaction.

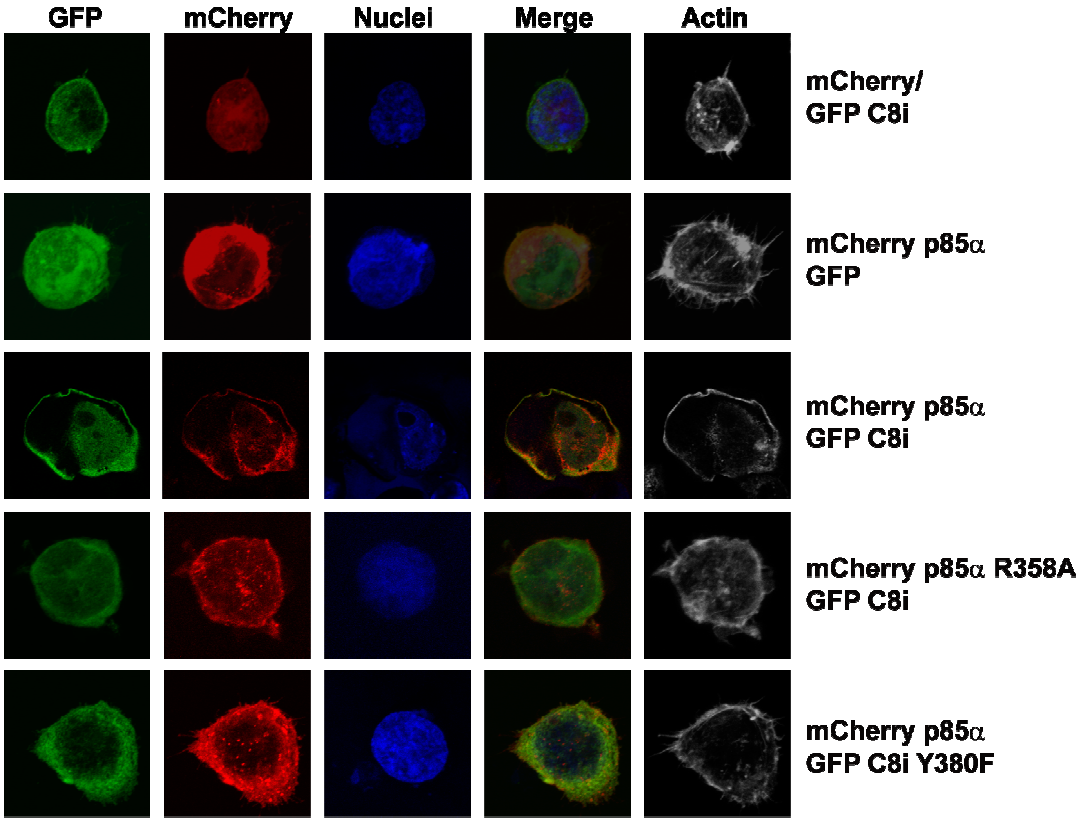

Figure 12: Intracellular colocalization of p85α and caspase-8

Confocal images were taken at 100x HEK 293T cells were transiently transfected with GFP-tagged C8i mutants or mCherry-tagged p85α mutants. Actin and nuclei were stained with phalloidin and DAPI, respectively.

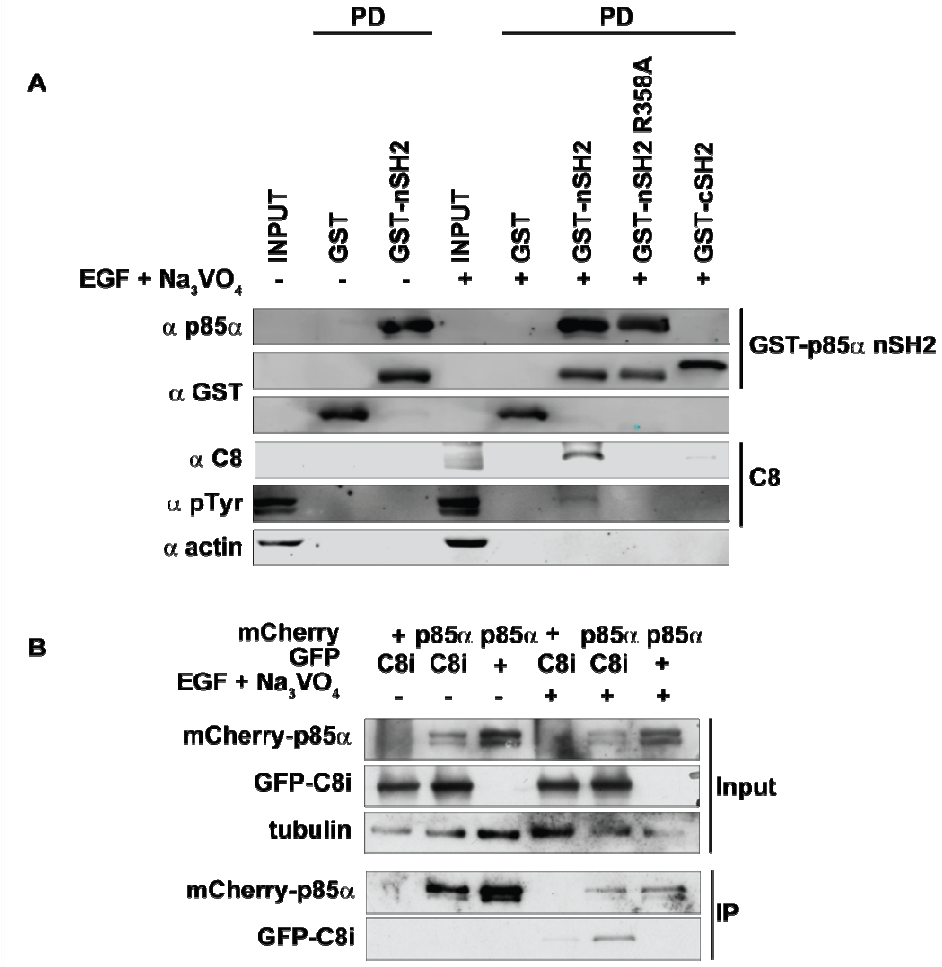

Figure 13: Caspase-8 and p85α form an intracellular complex

A) HEK293T colocalization B) Pull down (PD) using GST SH2 fusion proteins in OVCAR5 cells. C) IP of SKOV3 mCherry p85α and caspase-8

To examine complex formation with full length p85α intracellularly, the ovarian cancer cell line SKOV3 was stably transfected with mCherry alone or mCherry-tagged p85α along with GFP alone or GFP-tagged inactive caspase-8 (Figure 13 B). Non-stimulated and EGF stimulated stable SKOV3 cell lysates were immunoprecipitated with mCherry antibody. While caspase-8 p85α complex formation was not detected in non-

stimulated cells, GFP-tagged caspase-8 was pulled down in phosphorylation stimulated cells that had exogenous mCherry-tagged p85a. Thus our results conclude that intracellularly, the nSH2 domain of p85 is responsible for interacting with caspase-8 and R358 is indispensable for this interaction.

Caspase-8 promotes adhesion in ovarian cancer cells

Previous studies in neuroblastoma cells have shown that caspase-8 enhances cell adhesion dependent on Y380 and independent of catalytic activity of caspase-8 [2]. To investigate whether this finding is reflected in ovarian cancer cells, OVCAR5 caspase-8 knockdowns were reconstituted with either inactive caspase-8 or inactive caspase-8 Y380F (Figure 14 A). Subsequently, these OVCAR5 caspase-8 mutants were assessed for adhesion to fibronectin (Figure 14 B, C). In accordance with previous studies, OVCAR5 knockdown of endogenous caspase-8 reduced adhesion. However, reconstitution of inactive caspase-8 with and without mutated Y380 did not rescue adhesion.

To further investigate caspase-8's role in adhesion, we aimed at establishing a caspase-8 knockdown in SKOV3 cells (Figure 12 D, E). Interestingly, generation of stable knockdowns was not feasible. Upon selection for stable cell knockdown of caspase-8 over days 3-7 days, cells underwent morphological changes and became more rounded, eventually detaching from the plate after 7 days. Cells that lost their adhesion ability were found to be 69.35% ± 3.62% viable, indicating that detachment was not due to an increase in cell death but rather to a decrease in adhesion.

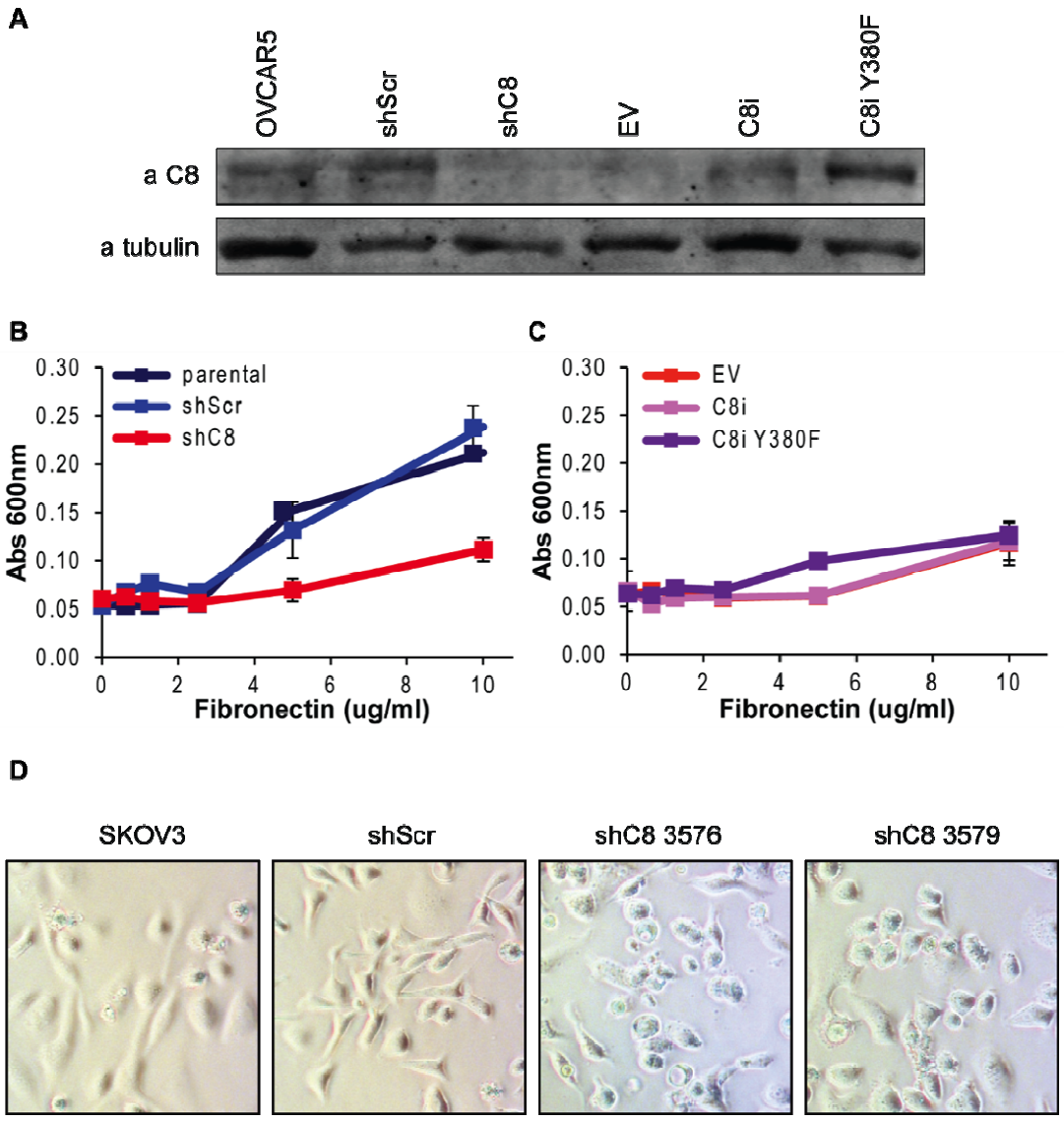

Figure 14: Caspase-8 promoting cell adhesion

A) Western blot of caspase-8 in OVCAR5 caspase-8 mutant cell lines. B) OVCAR5 adhesion to fibronectin (2ug/ml) C8 indicates overexpression of active caspase-8. C8i indicates reconstitution of inactive (C360A) caspase-8 mutants. D) SKOV3 knockdown of caspase-8 affect adhesion to plate, detaches cells with western blot. Images taken 5 days post infection.

Caspase-8 does not affect PI3K dependent AKT activation

Since our data demonstrates that caspase-8 and p85α interact, we next examined the interaction affects the regulatory ability of p85α on p110α, the catalytic subunit of PI3K. To test for PI3K activity, we detected activation of AKT by comparing Ser473 phosphorylated AKT versus total AKT by Western blot (Figure 15). Preliminary data of EGF stimulated OVCAR5 cells probed for S473 phosphorylation of AKT showed no obvious trends relating caspase-8 expression with AKT phosphorylation. However, further experiments are required to confirm these findings.

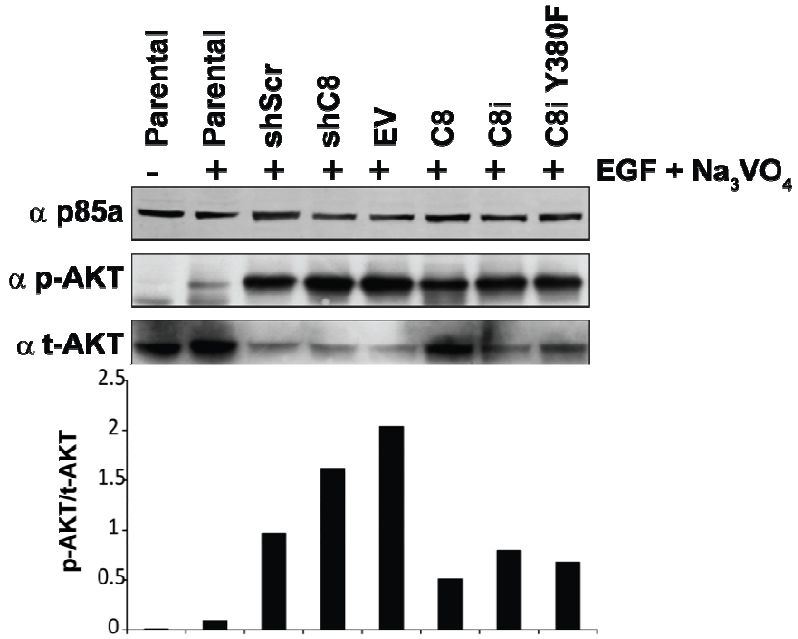

Figure 15: Caspase-8 no effect on PI3K activity

Western blot probed for AKT phosphorylation of Ser473 versus total AKT was used as a readout for PI3K activity. Ratio of Ser473 AKT versus total AKT quantified.

DISCUSSION

The n-terminal SH2 domain of p85α interacts with caspase-8

Previously, Senft and colleagues described an interaction between caspase-8 and p85α though the cSH2 domain of p85α [2]. They used a phosphorylated peptide sequence that corresponds to the intersubunit region of caspase-8 containing Y380 to bind a dot array of various SH2 domains. Their analysis of the data indicates that the cSH2 domain of p85α (p85-D2) was a strong candidate for binding. However, preliminary data in our lab using the same dot array of SH2 domains and a Src-phosphorylated inactive catalytic domain of capsase-8 suggested that the initial screen done by Senft et al. was misaligned (unpublished data). Careful alignment of our screen as well as realignment of the Senft screen identifies that phosphorylated caspase-8 binds to the nSH2 domain of p85α and p85β, respectively. Validating this possibility, ELISA data that screened for Src-phosphorylated capsase-8 binding against 11 purified SH2 domains indicated that the nSH2 domain of p85α was a strong interactor (Figure 9). Additional ELISAs and pull down experiments using ovarian cancer cells comparing the binding of the nSH2 versus the cSH2 domain of p85α to phosphorylated caspase-8 clearly indicate that caspase-8 binds to the nSH2 domain of p85α (Figure 9 D, E, 2.4 B). Furthermore, mutating the stabilizing arginine (R358A) in the phosphotyrosine pocket of the nSH2 domain abrogated binding to caspase-8 at Y380 in ELISAs and pull down experiments (Figure 9 F, 2.4 B), which supports a canonical interaction . Prior work demonstrated that deletion of the cSH2 domain in p85α abolished interaction with caspase-8 compared to wild type p85α in neuroblastoma cells [2]. However, the strategy is somewhat flawed as deletion of

an entire domain can alter the overall folding and structure of p85α, which may disrupt binding in and of itself.

Collectively, a combination of ELISA (Figure 9), NMR spectroscopy (not shown, unpublished results), confocal microscopy, pull down, and immunoprecipitation (Figure 12) determined the domains and specific residues critical for the interaction between caspase-8 and p85α. All experiments led to the same conclusion that the nSH2 domain of p85α is binding to the catalytic domain of caspase-8 and this interaction is dependent on R358 of p85α and phosphorylated Y380 of caspase-8. Binding of the cSH2 in ELISA experiments or pull down studies was not detected.

Biological implications of interaction between caspase-8 and p85α

Phosphorylation of caspase-8 at Y380 has previously been implicated in regulation of its enzymatic maturation [25, 32]. Typically, caspase-8 autoprocesses itself by cleaving the flexible intersubunit linker and removing a fragment that contains the Y380, in turn exposing the active site of caspase-8. Phosphorylation at Y380 might induce conformation changes in the linker or sterically hinder access to the cleavage motifs within the linker at D374 and D384 [25, 26]. In addition, phosphorylation at Y380 seems to provide a new interaction surface for protein-protein interaction, in particular with SH2 domains. The Y380 region of caspase-8 (YELM) is concordant with the specificity motif (YXXM) for SH2 domains of p85α [38]. To better understand the influence of binding of the nSH2 of p85α to the linker region of caspase-8 we modeled a putative complex by aligning the Y380 region of caspase-8 with a phosphopeptide bound to the nSH2 of p85α (Figure 16). Whereas this model may not reflect actual binding

interactions it strongly indicates that formation of the complex retains caspase-8 in its unprocessed conformation by covering the cleavage motifs within the intersubunit linker. So far, prevention of caspase-8 processing has been linked to keeping the protein in its inactive conformation [39, 40]. However, we cannot exclude that binding might induce drastic conformational changes of the linker, thereby exposing the active site of caspase-8. Further structural analysis would be needed to shed light on the how binding of p85α affects the conformation and activation of caspase-8.

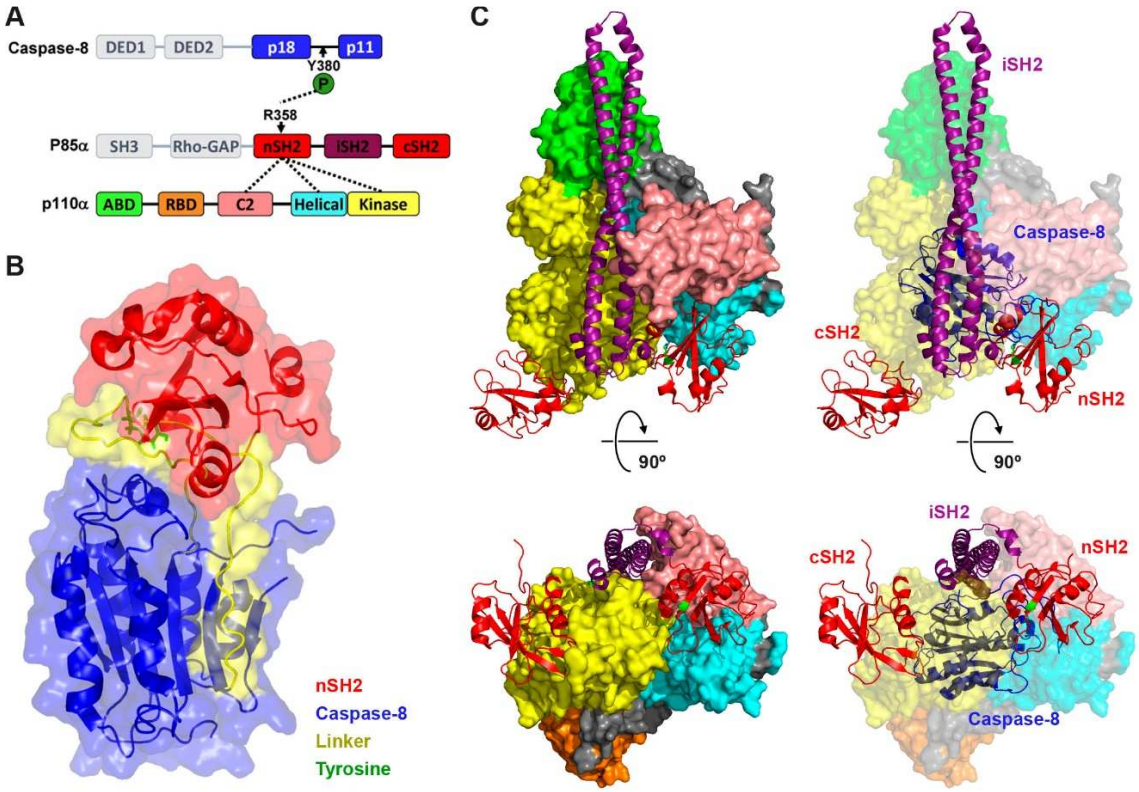

Figure 16: Models of capsase-8 p85α interaction

A) Domain map interaction of caspase-8, p85α, and p110α. B) Model of caspase-8 monomer (PDB: 2K7Z) and nSH2 domain bound to a phosphotyrosine peptide (PDB:2IUG). C) Model of nSH2-iSH2-cSH2 fragment of p85α bound to p110α (left). Model of caspase-8 (blue) bound to the nSH2 domain of p85α, while in complex p110α (faded) (right).

Caspase-8 binding to p85α potentially influences PI3K activity

In addition to regulating caspase-8 activation, p85α binding to caspase-8 may affect their subsequent interaction with other proteins. Regulating PI3K activity, p85α forms a heterodimer with the catalytic p110α subunit of the kinase (Figure 16 A, C). Previous structures indicate that the nSH2 interacts with the C2, helical, and kinase domains of p110α. According to our studies, capase-8 interacts via Y380 with the nSH2 at R358 located in the phosphotyrosine pocket. However, a crystal structure of the p110α in complex with the nSH2-iSH2 fragment of p85α reveals that this pocket this pocket faces p110α and is not available for further interactions. Therefore, simultaneous binding of caspase-8 and p110α to the nSH2 domain of p85α is not possible without inducing major conformational changes occurring (Figure 16 C).

The nSH2 domain of p85α is specifically required to inhibit and stabilize the heat sensitive and easily degraded catalytic subunit of PI3K p110α, as evidenced by reduced p110α expression when p85α is homozygously deleted [41]. Based on our structural model, the binding of caspase-8 to the nSH2 domain might induce conformational changes between p85α and p110α resulting in potential dissociation and degradation of p110α.

Alternatively, p85α interaction with caspase-8 could influence p110α activity. Typically, upstream signals activate tyrosine receptor kinases to autophosphorylate (i.e. PDGFR (platelet derived growth factor receptor)) or phosphorylate adaptor proteins (ie. IRS-1/2 (insulin receptor substrates)). Often these phosphotyrosines provide interaction sites for the SH2 domains of p85α, effectively recruiting p85α/p110α dimers to the

plasma membrane and activating p110α to phosphorylate $PI(4,5)P_2$ to $PI(3,4,5)P_3$. Multiple studies as well as the confocal analysis described in this work have shown that caspase-8 is also recruited to the membrane in a Y380 dependent manner [5, 42, 43] (Figure 12. Therefore, caspase-8 interaction with the nSH2 domain of p85α most likely affects its PI3K activity at the membrane and downstream signaling via effector molecules like AKT, RAC, GSK3, GEFs, GAPs, etc. (reviewed in [37]). Preliminary experiments in OVCAR5 cells could not detect significant caspase-8 dependent changes in AKT Ser473 phosphorylation within one hour of EGF stimulation (Figure 15), which is concurrent with results by Senft et al. obtained in in neuroblastoma cells [2]. However, the influence of caspase-8 on PI3K activity may be time dependent and affect the kinetics of AKT phosphorylation at Ser473 at shorter or longer time points than the here tested 1 hour. Moreover, phosphorylation of AKT on Ser473 may be an insufficient read out for PI3K activity, since AKT activation requires phosphorylation of Thr308 and additional phosphorylation of Ser473 only maximizes activity. AKT could be phosphorylated on Ser473, but not be activated if Thr308 is not phosphorylated. Even if we could not detect an effect on downstream AKT signaling, caspase-8 might influence other PI3K dependent pathways that are initiated by other effector molecules. A more thorough investigation is necessary to determine how caspase-8 interplays with the multitude of PI3K pathways.

Caspase-8 recruitment to early endosomes by binding to a p85α Rab5 complex

Additional membrane interactions of p85α and caspase-8 were shown to be involved in the activation of Rab5, a small GTPase in neuroblastoma cells [2, 43]. These

findings describe a model in which Y380 of caspase-8 is critical for interacting with the SH2 domains of p85α, which affects the ability of the GAP domain of p85α to regulate Rab5 activity and in turn promote integrin trafficking, there by potentially affecting cell migration. Torres et al. found that caspase-8 expression induced localization of Rab5 and accumulation of early endosomes at the cell periphery. This phenomenon did not require activity of caspase-8, but did require Y380 in neuroblastoma cells. While our staining of p85α and caspase-8 did not appear to specifically indicate accumulation of caspase-8 to early endosomes at the periphery, additional staining of caspase-8 and p85α with Rab5 or other endosome proteins are needed to validate any physical association. Whether caspase-8 regulation of Rab5 and endosomal trafficking affects cell migration in ovarian cancer has yet to be determined.

Caspase-8 and p85α affecting adhesion and migration

Previous studies have linked phosphorylated of caspase-8 to non-apoptotic functions such as cell adhesion and migration [2, 4, 5, 31, 43, 44]. Direct association of p85α to β-catenin in the cadherin-based adhesion complex was described by Woodfield et al [44]. Remarkably, upon the expression of src in fibroblasts, the β-catenin interaction with p85α was partially reduced. Extensive dissociation, yeast hybrid analysis, and pull downs demonstrated that β-catenin directly bound to the nSH2 domain of p85α. Since β-catenin does not have any matching YXXM motifs, the phosphotyrosine pocket of the nSH2 domain of p85α may be accessible for other protein-protein interactions. Perhaps the src induced diminished p85α β-catenin interaction may be attributed to a src phosphorylated caspase-8 binding to the phosphotyrosine pocket the p85α nSH2 domain

that we have shown (Figure 9 F). Disruption of a p85α interaction with the cadherin-based adhesion complex via β-catenin may have effects on cell adhesion.

While the effect of p85α interacting with β-catenin in adhesion complexes is yet to be determined, the involvement of phosphorylated caspase-8 in cell adhesion and migration has been well established in neuroblastoma cells [2, 4, 5, 44]. In fact, data from the src phosphorylated caspase-8 SH2 binding screen (Figure 9) was used as support to demonstrate that Src-phosphorylated caspase-8 can promote migration when interacting with the SH2 domain of CrkL at the cell periphery in [5]. Furthermore, Barbero et al. and Senft et al. identified that the Y380 of caspase-8 interacts with SH2 domains and is critical for localizing caspase-8 to the cell periphery and mediating cell migration and adhesion that is independent of catalytic activity in neuroblastoma cells [2, 4]. Here in OVCAR5 and SKOV3 cells, knockdown of caspase-8 seemed to also reduce cell adhesion (Figure 14). Especially in SKOV3 cells, caspase-8 seems to be absolutely required for proper cell adhesion. This may be attributed to a somatic mutation in the p110α catalytic subunit of PI3K (H1047R), which is known to be more catalytically active. Previous studies have shown that while the H1047R p110α mutant has higher activity compared to wild type, the H1047R mutant can still be regulated by p85α, specifically by the nSH2-iSH2 domains [45].

Interestingly, the decrease in adhesion in OVCAR5 cells was dependent upon caspase-8 activity and independent of Y380 (Figure 14 A-D). This discrepancy may be attributed to the fact that the neuroblastoma cell line used (NB7) lack endogenous caspase-8, allowing for cleaner examination of the effect of caspase-8, whether wild-type or mutated. Even though endogenous caspase-8 is knocked down in the ovarian cancer

cell models used in this study, it is still expressed at low levels. The transfected inactive caspase-8 mutants potentially dimerize with endogenous caspase-8, thereby activating it. This would lead to the processing of the inactive exogenous caspase-8 and subsequent removal of its intersubunit linker containing Y380.

Conclusions

Previous studies have demonstrated non-apoptotic roles of caspase-8 in cellular functions that contribute to metastasis; however, much of these studies have been done in neuroblastoma or neutrophil cell models. This thesis characterizes the interaction between caspase-8 and p85α and investigates the interaction in ovarian cancer. These results indicate that caspase-8 and p85α interact by Y380-dependent binding of caspase-8 to the nSH2 domain of p85α in ovarian cancer cells. In addition, caspase-8 appears to promote adhesion in these cells, but potentially in a manner that is independent of the Y380 site. A model of a caspase-8/p85α/p110α complex indicates that caspase-8 interaction with p85α may have biological implications for PI3K signaling. Understanding the interaction between caspase-8 and p85α may clarify mechanisms by which some of caspase-8's dual roles are regulated, providing insight into the paradoxical retention of the caspase during tumor progression, as well as for therapies directed at optimizing tumor cell death.

APPENDIX

General

10X TBS (2L)
121.1g Tris base
175.3g NaCl
pH 7.4 HCL

TBST
20mM Tris pH 7.6
0.1% Tween-20
0.123M NaCl
pH 7.6

PBST
1X PBS (Invitrogen)
0.1% Tween-20

ELISA

4x Src Buffer
20mM PIPES pH 7
10mM MnCl2
0.1mM TCEP
2mM ATP

Blocking buffer
5% milk in TBST

GST Protein Purification

High salt buffer
100mM Tris pH 8.0
300mM NaCl

Elution Buffer
20mM reduced glutathione

100mM Tris pH 8.0
120mM NaCl

Adhesion Assay

Crystal Violet Staining (10ml)
2ml 0.5% Crystal violet in MeOH

1.5M NaCL

EGF Stimulation media
1nM Na_3VO_4
0.2% of 30% H_2O_2
50ng/ml epidermal growth factor (EGF)

Western Blotting

6X Reducing Buffer (10ml)
3.75 ml 1M Tris-HCL pH 6.8
0.6g SDS
4.8ml 100% mercaptoethanol
3mg bromophenol blue

5x Running Buffer (8L)
120.8g Tris base
576g Glycine
40g SDS

5x Transfer Buffer (8L)

116g Tris base
580g Glycine
20g SDS

Transfer Buffer (750ml)

20% 5X Transfer buffer
20% Methanol

Blocking Buffer
0.1% Casein in PBS
5% Milk in TBST

RIPA buffer
0.1M Tris-Base-HCl pH 8
150nM NaCl
1mM EDTA
1% Deoxycholic acid
1% Triton X-100
0.1% SDS
1% Protease inhibitor cocktail (Sigma)
0.4% 0.5M Na_3VO_4
5% 1M NaF

REFERENCES

1. Fulda, S., *Caspase-8 in cancer biology and therapy.* Cancer Lett, 2009. **281**(2): p. 128-33.

2. Senft, J., B. Helfer, and S.M. Frisch, *Caspase-8 interacts with the p85 subunit of phosphatidylinositol 3-kinase to regulate cell adhesion and motility.* Cancer Res, 2007. **67**(24): p. 11505-9.

3. Stupack, D.G., *Caspase-8 as a therapeutic target in cancer.* Cancer Lett, 2010. **332**(2): p. 133-40.

4. Barbero, S., et al., *Identification of a critical tyrosine residue in caspase 8 that promotes cell migration.* J Biol Chem, 2008. **283**(19): p. 13031-4.

5. Graf, R., et al., *Src-inducible association of CrkL with procaspase-8 promotes cell migration.* Cell Adh Migr, 2013. **7**(4): p. 362-9.

6. Society, A.C., *Cancer Facts & Figures 2014*. 2014: Atlant.

7. Society, A.C., *The History of Cancer*. 2014.

8. Sudhakar, A., *History of Cancer, Ancient and Modern Treatment Methods.* J Cancer Sci Ther, 2009. **1**(2): p. 1-4.

9. Watson, J.D. and F.H. Crick, *Molecular structure of nucleic acids: a structure for deoxyribose nucleic acid. J.D. Watson and F.H.C. Crick. Published in Nature, number 4356 April 25, 1953.* Nature, 1974. **248**(5451): p. 765.

10. Siegel, R., et al., *Cancer statistics, 2014.* CA Cancer J Clin, 2014. **64**(1): p. 9-29.

11. Institute, N.C. *Metastatic Cancer* National Cancer Institute: Fact Sheet [web page] 2013 3/28/2013 [cited 2014; Available from: http://www.cancer.gov/cancertopics/factsheet/Sites-Types/metastatic.

12. Ando, K., et al., *Molecular alterations associated with osteosarcoma development.* Sarcoma, 2012. **2012**: p. 523432.

13. Society, A.C. *Ovarian Cancer*. [Web page] 2013 2/6/2014 [cited 2014; Available from: http://www.cancer.org/acs/groups/cid/documents/webcontent/003130-pdf.pdf.

14. Howlader N, N.A., Krapcho M, Garshell J, Miller D, Altekruse SF, Kosary CL, Yu M, Ruhl J, Tatalovich Z, Mariotto A, Lewis DR, Chen HS, Feuer EJ, Cronin KA (eds), *SEER Cancer Statistics Review, 1975-2011*. 2011, National Cancer Institute: Bethesda, MD.

15. Shield, J.P., et al., *Management and 1 year outcome for UK children with type 2 diabetes.* Arch Dis Child, 2009. **94**(3): p. 206-9.

16. Helm, W.E., RP. *Ovarian Cancer Staging*. [web page] 2013 5/21/13 [cited 2014; Available from: http://emedicine.medscape.com/article/2007140-overview.

17. Goff, B.A., et al., *Ovarian carcinoma diagnosis.* Cancer, 2000. **89**(10): p. 2068-75.

18. Armstrong, D.K., et al., *Intraperitoneal cisplatin and paclitaxel in ovarian cancer.* N Engl J Med, 2006. **354**(1): p. 34-43.

19. McCreath, W.A. and D.S. Chi, *Surgical cytoreduction in ovarian cancer.* Oncology (Williston Park), 2004. **18**(5): p. 645-53, discussion 653-4, 656, 658.

20. Dasari, S. and P. Bernard Tchounwou, *Cisplatin in cancer therapy: Molecular mechanisms of action.* Eur J Pharmacol, 2014.

21. Bast, R.C., Jr., B. Hennessy, and G.B. Mills, *The biology of ovarian cancer: new opportunities for translation.* Nat Rev Cancer, 2009. **9**(6): p. 415-28.

22. Kar, R., et al., *Role of apoptotic regulators in human epithelial ovarian cancer.* Cancer Biol Ther, 2007. **6**(7): p. 1101-5.

23. Mattson, M.P., *Apoptosis in neurodegenerative disorders.* Nat Rev Mol Cell Biol, 2000. **1**(2): p. 120-9.

24. Muzio, M., et al., *FLICE, a novel FADD-homologous ICE/CED-3-like protease, is recruited to the CD95 (Fas/APO-1) death--inducing signaling complex.* Cell, 1996. **85**(6): p. 817-27.

25. Keller, N., M.G. Grutter, and O. Zerbe, *Studies of the molecular mechanism of caspase-8 activation by solution NMR.* Cell Death Differ, 2010. **17**(4): p. 710-8.

26. Keller, N., et al., *Structural and biochemical studies on procaspase-8: new insights on initiator caspase activation.* Structure, 2009. **17**(3): p. 438-48.

27. Muzio, M., et al., *An induced proximity model for caspase-8 activation.* J Biol Chem, 1998. **273**(5): p. 2926-30.

28. Cory, S. and J.M. Adams, *The Bcl2 family: regulators of the cellular life-or-death switch.* Nat Rev Cancer, 2002. **2**(9): p. 647-56.

29. Varfolomeev, E.E., et al., *Targeted disruption of the mouse Caspase 8 gene ablates cell death induction by the TNF receptors, Fas/Apo1, and DR3 and is lethal prenatally.* Immunity, 1998. **9**(2): p. 267-76.

30. Helfer, B., et al., *Caspase-8 promotes cell motility and calpain activity under nonapoptotic conditions.* Cancer Res, 2006. **66**(8): p. 4273-8.

31. Barbero, S., et al., *Caspase-8 association with the focal adhesion complex promotes tumor cell migration and metastasis.* Cancer Res, 2009. **69**(9): p. 3755-63.

32. Cursi, S., et al., *Src kinase phosphorylates Caspase-8 on Tyr380: a novel mechanism of apoptosis suppression.* Embo J, 2006. **25**(9): p. 1895-905.

33. Liu, B.A., B.W. Engelmann, and P.D. Nash, *The language of SH2 domain interactions defines phosphotyrosine-mediated signal transduction.* FEBS Lett, 2012. **586**(17): p. 2597-605.

34. Waksman, G., et al., *Crystal structure of the phosphotyrosine recognition domain SH2 of v-src complexed with tyrosine-phosphorylated peptides.* Nature, 1992. **358**(6388): p. 646-53.

35. Jia, S.H., et al., *Dynamic regulation of neutrophil survival through tyrosine phosphorylation or dephosphorylation of caspase-8.* J Biol Chem, 2008. **283**(9): p. 5402-13.

36. Mellor, P., et al., *Multiple roles for the p85alpha isoform in the regulation and function of PI3K signalling and receptor trafficking.* Biochem J, 2012 **441**(1): p. 23-37.

37. Vanhaesebroeck, B., L. Stephens, and P. Hawkins, *PI3K signalling: the path to discovery and understanding.* Nat Rev Mol Cell Biol, 2012. **13**(3): p. 195-203.

38. Songyang, Z., et al., *SH2 domains recognize specific phosphopeptide sequences.* Cell, 1993. **72**(5): p. 767-78.

39. Donepudi, M., et al., *Insights into the regulatory mechanism for caspase-8 activation.* Mol Cell, 2003. **11**(2): p. 543-9.

40. Pop, C., et al., *Role of proteolysis in caspase-8 activation and stabilization.* Biochemistry, 2007. **46**(14): p. 4398-407.

41. Yu, J., et al., *Regulation of the p85/p110 phosphatidylinositol 3'-kinase: stabilization and inhibition of the p110alpha catalytic subunit by the p85 regulatory subunit.* Mol Cell Biol, 1998. **18**(3): p. 1379-87.

42. Graf, R.P., et al., *Caspase-8 as a regulator of tumor cell motility.* Curr Mol Med, 2014. **14**(2): p. 246-54.

43. Torres, V.A., et al., *Caspase 8 promotes peripheral localization and activation of Rab5.* J Biol Chem, 2008. **283**(52): p. 36280-9.

44. Woodfield, R.J., et al., *The p85 subunit of phosphoinositide 3-kinase is associated with beta-catenin in the cadherin-based adhesion complex.* Biochem J, 2001. **360**(Pt 2): p. 335-44.

45. Backer, J.M., *The regulation of class IA PI 3-kinases by inter-subunit interactions.* Curr Top Microbiol Immunol, 2010. **346**: p. 87-114.